Microchimica Acta (2018) 185: 459
https://doi.org/10.1007/s00604-018-2998-9

ORIGINAL PAPER

A glassy carbon electrode modified with nitrogen-doped reduced graphene oxide and melamine for ultra-sensitive voltammetric determination of bisphenol A

Jingyu Qin[1] · Jing Shen[1] · Xiangyang Xu[1] · Yuan Yuan[1] · Guangyu He[1] · Haiqun Chen[1]

Received: 15 June 2018 / Accepted: 8 September 2018 / Published online: 15 September 2018

Abstract

A composite was prepared at room temperature from nitrogen-doped reduced graphene oxide (N-rGO) and melamine via π-interaction. An ultra-sensitive electrochemical sensor for the determination of trace levels of bisphenol A (BPA) was obtained by coating a glassy carbon electrode (GCE) with the composite. The structure and morphology of composite were characterized by FTIR, Raman, XRD, XPS, SEM and TEM. Because of the synergetic effects of N-rGO and melamine, the modified GCE displays considerably enhanced sensitivity to BPA. The voltammetric response, typically measured at a peak of 0.48 V (vs. SCE) is linear in the 0.05 to 20 μM BPA concentration range, and the detection limit is 0.8 nM (at $S/N = 3$). The sensor is reproducible, stable and selective. It was applied to analyze baby bottles, drinking cups, mineral water bottles and shopping receipts that were spiked with BPA, and the recoveries reached 99.1–101.4%.

Keywords Carbon-based nanomaterials · π-Interaction · Supramolecular system · Sensor · Voltammetry · Differential pulse voltammetry · Real sample analysis · Endocrine disruptor · Trace BPA · Electrochemical detection

Introduction

Various analytical methods have been established for detecting trace bisphenol A (BPA) in water, such as fluorimetry [1], gas chromatography-mass spectrometry [2], liquid chromatography-mass spectrometry [3] and electrochemical sensor [4], etc. Compared with other approaches, electrochemical methods present advantages owing to its excellent sensitivity, prominent selectivity and simple operation [5].

Generally, enzyme [4], metal nanoparticles [6], and carbon-based materials [7] are applied to increase the analytical response of electrochemical sensors. Among these electrode materials, enzymes are commonly used as biosensors due to good biological compatibility. Nanoparticles of metal oxide (NiO [8], Fe_3O_4 [9]) or noble metals (AuNPs [10], PtNPs [11]) are the conventional candidates in the field of electrochemistry. Thanks to the properties of size controllability, chemical stability and high catalysis activity, it is very advantageous for them to be applied in sensors [11]. Nevertheless, ameliorating the shortcomings of nanoparticles including high costs, low surface area and easy agglomeration are still challenging.

Carbon-based materials stand out because of their excellent electrocatalytic properties and strong adsorption capacity for analytes. Graphene, a two-dimensional carbon nanomaterial with honeycomb-structure, has shown unique advantages in the construction of electrochemical sensors. Studies have proved that N-doped graphene possesses a better electrical conductivity and large amounts of edge sites than graphene [12]. And its superiority of high surface area and catalytic ability has captured great interest. Melamine were introduced during the modification of sensors because of its unique benzene ring-structure. In addition, protonated melamine adsorbs negatively

Electronic supplementary material The online version of this article (https://doi.org/10.1007/s00604-018-2998-9) contains supplementary material, which is available to authorized users.

✉ Guangyu He
hgy610@hotmail.com

✉ Haiqun Chen
hqchenyf@hotmail.com

[1] Key Laboratory of Advanced Catalytic Materials and Technology, Advanced Catalysis and Green Manufacturing Collaborative Innovation Center, Changzhou University, Changzhou, Jiangsu Province 213164, China

charged BPA to the surface of electrode more easily, which can effectively improve the sensitivity of the sensor. Based on the above properties, we have reason to believe that nitrogen-doped reduced graphene oxide (N-G) can self-assemble with melamine to form a supramolecular system through π-interaction. The introduction of melamine provides rigid support for N-G and allows it to stack orderly [13]. The synergistic effect between N-G and melamine enhances electron transfer rate, leading to a higher current response to BPA.

In this paper, nitrogen-doped reduced graphene oxide /melamine (N-G/M) modified glassy carbon electrode (GCE) was used to construct successfully an original electrochemical sensor for detecting BPA. Here, melamine plays a role as modifier. The electrochemical performance of N-G/M modified GCE was studied by cyclic voltammetry. The sensitivity of the electrode was proved by kinetic calculation, and the detection limit was evaluated to be nearly one order of magnitude lower than those reported in other literatures [14–16].

Experimental

Materials

Natural graphite powder (99.9%, 500mesh), melamine, BPA, Na_2HPO_4, NaH_2PO_4 were purchased from Sinopharm Chemical Reagent Co. Ltd. (China, www.labgogo.com). All materials were of analytical grade and used directly without further purification. Ultrapure water was used throughout the experiments.

Characterization

X-ray diffraction (XRD) patterns were performed on a Bruker D/max 2500 PC X-ray diffractometer (Rigaku, Japan) with Cu Kα radiation (λ = 0.15418 Å) at the scanning angle ranging from 5° to 70°. The morphology and microstructure of prepared composite were characterized by SUPRA55 field emission scanning electron microscopy (FE-SEM, Zeiss, Germany) and JEM-2100 transmission electron microscopy (TEM, JEOL, Japan). Fourier transform infrared (FTIR) spectroscopy studies were conducted by a Nicolet iS50 spectrometer (Thermo, USA) with the scanning range of 450–4000 cm^{-1}. Raman spectra were analyzed using RM1000-Invia Reflex Raman microprobe (Renishaw, U.K). X-ray photoelectron spectroscopy (XPS) were taken by a PHI-5000C ESCA system (PerkinElmer, USA) with Mg K_α radiation (hv = 1253.6 Ev).

All electrochemical measurements were recorded on the CHI 920 workstation (CH Instrument, Shanghai) with a three-electrode system in 0.1 M phosphate buffer (equal volume of 0.1 M NaH_2PO_4 and 0.1 M Na_2HPO_4). The working electrode was a modified GCE or a bare GCE, while a saturated calomel electrode (SCE, Hg/Hg_2Cl_2) was used as the reference electrode and a platinum wire was used as the auxiliary electrode.

Preparation of the nitrogen-doped reduced graphene oxide and melamine composite (N-G/M)

Graphite oxide (GO) was synthesized by modified Hummers' method [17]. And N-G was synthesized according to literature [18]. Then, equal volume (5 mL) of N-G suspension (1.0 mg/mL) and the melamine saturated solution (3.1 mg/mL) were mixed together and stirred for 1 h, then ultrasonicated for 30 min to form a dispersion of N-G/M (see detail in the electronic supporting material).

Preparation of the N-G/M-modified glassy carbon electrode (GCE)

Before use, GCE was first polished to a mirror-like surface and cleaned ultrasonically with ethanol and ultrapure water sequentially for 5 min. Afterward, the 15 μL of N-G/M suspension was coated onto the surface of dried GCE and heated stoving under an infrared lamp to form a stable film. The resulting modified electrode was denoted as N-G/M-GCE. Fabrication process of the electrochemical sensor for detecting BPA is illustrated in Scheme 1.

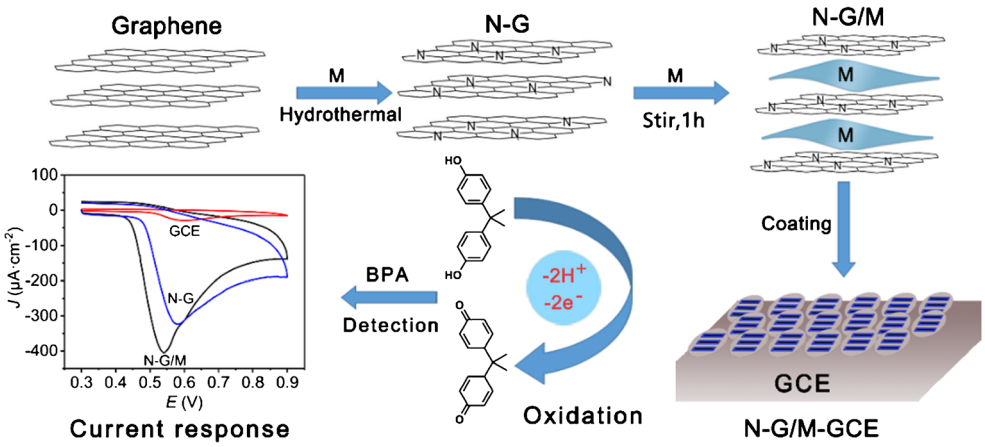

Scheme 1 Illustration of fabricating the electrochemical sensor for detecting BPA

Electrochemical measurements

The electrochemical impedance spectroscopy (EIS) was performed in 5 mM $[Fe(CN)6]^{3-/4-}$ containing 0.1 M KCl solution. The frequency range of EIS was from 0.01 to 10^5 Hz and initiative potential was adjusted at 0.25 V. The cyclic voltammetry was scanned with scan rate of 50 $mV{\cdot}s^{-1}$. The sample interval and quiet time of CV were set as 0.001 V and 2 s, respectively. Differential pulse voltammogram (DPV) was recorded from 0.3 to 0.9 V. The parameters were as follows: increment potential, 0.004 V; pulse amplitude, 0.05 V; pulse width, 0.0167 s; pulse period, 0.5 s; quiet time, 2 s.

Extraction of BPA from samples

To evaluate the practicality of the prepared sensor, N-G/M-GCE electrode was used for the actual sample analysis. The baby bottle (Pigeon), drinking cups (Lock & Lock), mineral water bottles (Wahaha) and shopping receipts were purchased from RT-MART (Changzhou, China) as experimental samples. BPA was extracted from the samples according to the literature [19]. Firstly, the samples were ultrasonicated with acetone and washed with ethanol and deionized water. After that, the cleaned plastic samples were cut into small pieces (2 g) and transferred into a flask equipped with a condenser, and then heated in 30 mL of deionized water at 70 °C for 48 h. Subsequently, the reaction mixture was filtered (Navigator Membrane Filter, pore size, 0.22 μm) and the filtrate was collected after cooling to ambient temperature. Finally, 4 mL of each filtrate was added to equal volume of phosphate buffer (pH = 7) and stored at low temperature before analysis.

Results and discussion

Choice of materials

Carbon-based materials, such as carbon dots, carbon nanotubes, graphene, have been successfully used to modify bare electrode [20]. However, the types of analytes carbon dots can detect are very limited [21]. And it is difficult for carbon nanotubes to be dispersed in routine solvents due to the intrinsic van der Waals interactions between pristine nanotubes [7]. In our previous studies [22], the highly ordered graphene paper with remarkable electrical conductivity, admirable thermal stability and excellent mechanical strength was successfully prepared, and used to improve the performance of electrochemical sensors. Nevertheless, it is difficult to control the conductivity of graphene owing to zero band gap, which limits its application in electrochemistry. Studies have proved that nitrogen doping can effectively adjust the energy band structure and modulate conducting types [23]. In addition, we assume that introducing benzene ring-structure materials to form a supramolecular system with N-G through π-interaction can further improve the conductivity of the electrochemical sensor. Compared with other heterocyclic compound, melamine stands out because it can be multi-protonated. During the procedure of detection, electrostatic interaction was involved between protonated melamine and negatively charged BPA, leading to a higher sensitivity of the sensor.

Characterization of composites

Melamine, N-G and N-G/M were analyzed by FTIR spectroscopy (Fig. 1a). The absorption peak of N-G at 1565 cm^{-1}

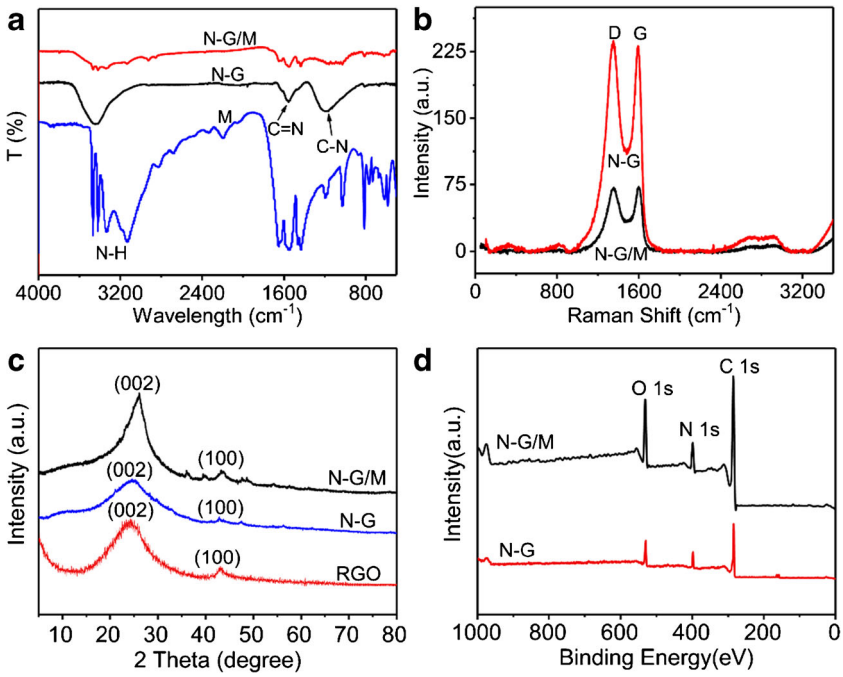

Fig. 1 **a** FTIR spectra of melamine, N-G and N-G/M. **b** Raman spectra of N-G and N-G/M. **c** XRD patterns of RGO, N-G, N-G/M. **d** Full XPS spectra of N-G and N-G/M

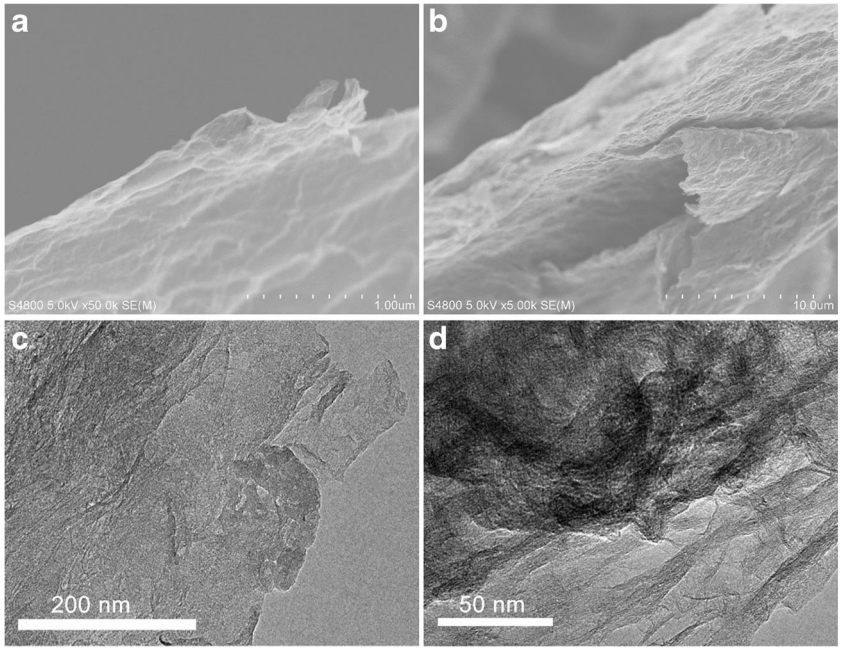

Fig. 2 Typical SEM images of (**a**) N-G and (**b**) N-G/M; TEM images of (**c**) N-G and (**d**) N-G/M

proves the existence of C=C bond. As expected, there are two new absorption peaks obtained at 1550 cm^{-1} and 1165 cm^{-1}, corresponding to the characteristic absorption peaks of C=N and C-N, respectively, which indicates that GO is doped with nitrogen [18, 24]. N-G/M exhibits a C=N stretching vibrational absorption peak of triazine ring between 1652 cm^{-1} and 1550 cm^{-1}, which coincides with the absorption peaks of C=N generated by N-doping of graphene. This result indicates that N-G/M is successfully prepared.

As shown in Raman spectra (Fig. 1b), the characteristic peaks of N-G appear at 1340 cm^{-1} and 1589 cm^{-1}, corresponding to the D and G band, respectively, whilst the G band of graphene is observed at 1580 cm^{-1}. This is due to the introduction of nitrogen atoms that causes a significant G band shift of N-G [25]. After combining with melamine, there is an obvious red shift of the D and G band of N-G/M composite. In addition, the Raman intensity of N-G/M is significantly weakened. That can be attributed to the fact that the surface of N-G is modified by melamine, causing decrease in the number of N-G sheets per unit volume [24]. The value for the D/G intensity ratio (I_D/I_G) of N-G ($I_D/I_G = 1.02$) is higher than that of N-G/M ($I_D/I_G = 0.99$), further indicating the lower defect density in N-G/M.

The typical XRD pattern (Fig. 1c) of N-G exhibits two peaks at $2\theta = 24.6°$ and $2\theta = 42.8°$, corresponding to (002) and (100) plane of reduced graphene oxide, respectively. This result indicates that N-G bears high resemblance in structure to graphene [26]. After the combination of N-G with melamine, the composite exhibits more sharp and intense diffraction peak corresponding to (002) plane. This might be because N-G sheets restack in an orderly manner due to the intercalation of melamine into the N-G layers, leading to high crystallinity.

Fig. 1d depicts full XPS spectra of N-G and N-G/M. The main peaks observed at 284 eV, 400 eV and 531 eV prove the coexistence of C 1 s, N 1 s and O 1 s in both materials. The intensities of characteristic peaks of N-G/M are stronger than

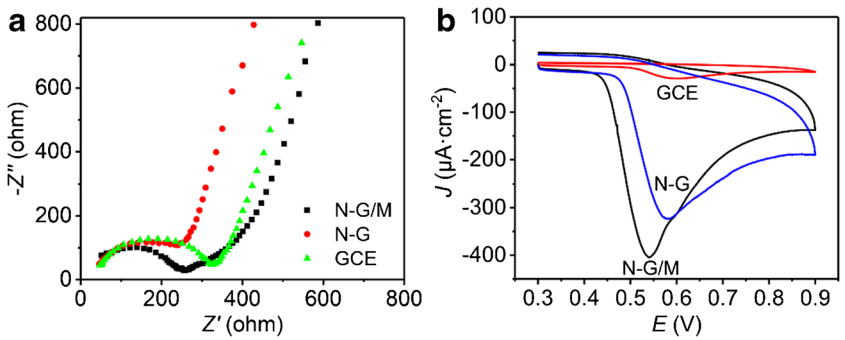

Fig. 3 **a** Nyquist plots of bare GCE, N-G-GCE and N-G/M-GCE in 5 mM $[Fe(CN)_6]^{3-/4-}$ containing 0.1 M KCl solution at an initiative potential of 0.25 V. **b** CV curves of bare GCE, N-G-GCE and N-G/M-GCE in 0.1 M phosphate buffer containing 25 μM BPA (voltage range:0.3 V–0.9 V; scan rate: 50 mV/s)

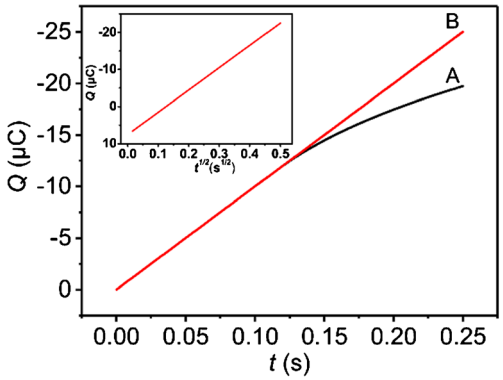

Fig. 4 Plot of Q-t curves on N-G/M-GCE in 0.1 M phosphate buffer (pH = 7.0) with (**a**), and without (**b**) 0.25 mM BPA, respectively; Calibration plot of Q-$t^{1/2}$ on N-G/M-GCE (Inset)

those of N-G, and the N percentage in N-G is estimated to be 9.95%, while the content in N-G/M is increased to 13.37% after the introduction of melamine.

The microstructure of N-G was investigated by SEM (Fig. 2a) and TEM (Fig. 2c). It can be clearly observed that N-G sheets have a transparent and crumpled silk-like morphology. SEM image (Fig. 2b) of N-G/M shows that it has a distinct lamellar texture. TEM image (Fig. 2d) presents clear shadowed areas, which further indicates that the melamine molecules are successfully immobilized to the surface of N-G by π stacking, and ushers the restack of N-G layer by layer simultaneously.

3.3 Electrochemical behavior of electrodes.

To further characterize the modified electrode, the electrochemical impedance spectroscopy (EIS) was obtained in the frequency range of 0.01–100,000 Hz. As shown in Fig. 3a, the diameter of the semicircle portion indicates the charge transfer resistance (R_{ct}) [27]. Besides, the impedance spectra of different working electrodes can be simplified by the Randles' equivalent circuit. The bare GCE shows a certain semicircle at high frequencies, and the R_{ct} value is about 326 Ω, indicating a high charge transfer resistance. The plot of N-G shows an obviously smaller radius with the R_{ct} value dramatically decreasing to 223 Ω. Furthermore, the easier electron transfer is involved when N-G/M is fixed on bare GCE. It might be due to the enhanced conductivity, which accelerates the transfer of electrons.

Figure 3b displays the cyclic voltammogram (CV) curves of bare GCE, N-G-GCE and N-G/M-GCE in 0.1 M phosphate buffer containing 25 μM BPA. A well-defined oxidation peak without reduction current peak is appeared at different electrodes in the selected potential window, suggesting an absolutely irreversible electrode reaction [28]. The N-G/M modified GCE exhibits higher current response for BPA oxidation (at 0.55 V) than bare GCE and N-G modified GCE. This is because melamine can be protonated at pH 7.0 (pK_a of melamine is 8) and become positively charged. Thanks to electrostatic interaction, the protonated melamine is more likely to adsorb negatively charged BPA to the surface of electrode [29], so the electrocatalytic activity and electron transfer rate of the sensor are improved.

In addition, the experimental conditions were optimized by CV test. The influence of pH on the oxidation of BPA at N-G/M-GCE proves that the transfer of electrons is accompanied by equal number of protons (Fig. S1). And the relationship between scan rate and the oxidation peak currents (Fig. S2) further demonstrates that two electrons and two protons are involved in the oxidation of BPA at N-G/M-GCE electrode. Therefore, the possible mechanism of the aptamer-captured BPA on prepared sensor is proposed as shown in Scheme S1.

Electrokinetics

The valid surface area of bare GCE and N-G/M-GCE were studied by chronocoulometry, and calculated according to Anson equation (eq. 1) [30]:

$$Q = 2nFAc\sqrt{\frac{Dt}{\pi}} + Qdl + Qads \quad (1)$$

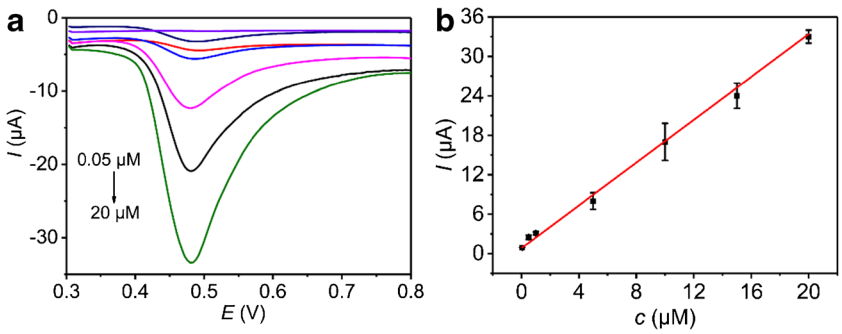

Fig. 5 **a** DPV curves for the detection of BPA at N-G/M-GCE with different concentrations (0.05, 0.5, 1, 5, 10, 15, 20 μM, respectively). **b** Linear calibration plot between BPA concentrations and the peak currents (working potential: 0.48 V vs. SCE), and the error bars correspond to the standard deviation ($n = 5$). Pulse amplitude, 0.05 V; pulse width, 0.0167 s; pulse period, 0.5 s

Table 1 Comparison of several fabricated sensors for detecting BPA

Electrode	Method	LDR(μM)	LOD(nM)	Reference
N-GS/CS-GCE[a]	Amperometry	0.01-1.3	5.0	[32]
TMO-GCE[c]	CV	0.8-7.2	1.2	[27]
PME/GR-CPE[b]	DPV	9.0-100.0	10.5	[33]
Ni_2Al LDH-GCE[d]	DPV	0.02–1.51	6.8	[34]
gold nanodendrites/GCE	DPV	0.05–55.0	1.2	[35]
N-G/M-GCE1	DPV	0.05–20.0	0.8	This work

[a] N-doped graphene sheets /chitosan composites modified GCE

[b] poly(melamine) coated graphene doped carbon paste electrode

[c] Ternary metal oxide (TMO) composite modified GCE

[d] Ni_2Al-layereddouble hydroxide nanosheets modified GCE

According to the calibration plot of Q-$t^{1/2}$ (Fig. S3), the calculated valid surface area (A) is 0.0097 cm^2 and 0.0998 cm^2 for bare GCE and N-G/M-GCE, respectively.

Faradic charge (Q_{ads}) and the diffusion coefficient (D) of BPA at N-G/M-GCE were obtained through chronocoulometry method in 0.1 M phosphate buffer with and without 0.25 mM BPA, respectively. As shown in the inset of Fig. 4, the calibration plot of Q vs. $t^{1/2}$ is described by the equation (eq. 2):

$$Q = -60.12 \times 10^{-6} \cdot t^{1/2} + 7.538 \times 10^{-6} \quad (2)$$

The intercept (Q_{ads}) is equal to 7.538×10^{-6} C. Then, according to the Anson equation, D is calculated to be 1.22×10^{-4} $cm^2 \cdot s^{-1}$ at room temperature. Additionally, the adsorption capacity (Γ_s) of BPA at N-G/M-GCE is calculated by the equation $Q_{ads} = nFA\Gamma_s$ to be 3.91×10^{-10} $mol \cdot cm^{-2}$ ($n = 2$, $A = 0.0998$ cm^2).

The standard heterogeneousrate constant (k_s) for N-G/M-GCE can be calculated by the Velasco equation (eq. 3) [31]:

$$k_s = 2.415 \exp(-002F/RT) D^{1/2} \left(E_{pa} - E_{pa/2}\right)^{-1/2} v^{1/2} \quad (3)$$

where E_{pa} stands for the peak potential and $E_{pa/2}$ represents the potential at $I = I_{pa/2}$. In this experiment, $D = 1.22 \times 10^{-4}$ $cm^2 \cdot s^{-1}$, $E_{pa/2}$-$E_{pa/2} = 30$ mV, $v = 50$ $mV \cdot s^{-1}$. As a result, k_s is calculated to be 1.58×10^{-2} $cm \cdot s^{-1}$ ($k_{s0} = 2.65 \times 10^{-3}$ $cm \cdot s^{-1}$), demonstrating a rapid electron transfer process.

Calibration features

The peak current response of N-G/M-GCE towards BPA in various concentrations was measured by differential pulse voltammetry (DPV). The oxidation peak current increases proportionally along with an increasing BPA concentration from 0.05 μM to 20 μM (Fig. 5a). And the fitting equation is expressed in Fig. 5d as I (μA) = $1.56787c + 1.096$ (R^2 = 0.9952). Consequently, the detection limit is obtained as 0.8 nM ($S/N = 3$). It indicates that N-G/M modified GCE possesses wide linear range for detecting BPA with high sensitivity (15.71 $\mu A \cdot \mu M^{-1} \cdot cm^{-2}$). That is benefited from the high electron transfer rate and electrocatalytic activity of N-G/M. Moreover, the protonated melamine helps adsorb negatively charged BPA onto the electrode surface through electrostatic interaction. The detection limit is much lower than that reported in literatures, which are presented in Table 1.

Repeatability, reproducibility, stability, and selectivity

To prove the accuracy of the modified electrode, the repeatability of the N-G/M-GCE carried out by cyclic voltammetry in 25 μM BPA. The relative standard deviation (RSD) was 2.5% for 8 successive measurements, which indicated the excellent repeatability of the fabricated sensor. The reproducibility was verified by detecting 25 μM BPA on six different N-G/M-GCE sensors with same fabrication procedures. All sensors exhibited similar current responses with the RSD of 2.8%. As for stability, the prepared electrode was stored in air for a week at ambient temperature. Only 3.7% decrease of current response with no shift of oxidation peak potential was observed, which revealed the good stability of the electrode.

Besides, the interference tests were carried out to estimate the selectivity of the prepared sensor under optimal conditions. Structures analogous (polyphenols etc.) and inorganic

Table 2 Interferences of other species on 25 μM BPA

Interferents	C (mol/L)	I_{pa} change (%)	Interferents	C (mol/L)	I_{pa} change (%)
Fe^{3+}	2.5×10^{-3}	−2.5	Phenol	1.25×10^{-3}	+4.3
Al^{3+}	2.5×10^{-3}	−2.9	Catechol	1.25×10^{-3}	+3.6
Mg^{2+}	2.5×10^{-3}	+3.1	Resorcinol	1.25×10^{-3}	+4.5
SO_4^{2-}	2.5×10^{-3}	−2.8	Hydroquinone	1.25×10^{-3}	+3.7
Cl^-	2.5×10^{-3}	−2.0	4-Nitrophenol	1.25×10^{-3}	+4.9

Table 3 Detection results in different samples

Samples	Measured[a] (μM)	Added (μM)	Found[a] (μM)	RSD[b] (%)	Recovery (%)
The baby bottles	11.4	11	22.2	4.1	99.1
Shopping receipt	17.1	11	28.5	2.3	101.4
Drinking cups	19.3	11	30.7	2.6	101.3
Mineral water bottles	22.8	11	34.2	3.4	101.2

[a] Average of three measurements

[b] Relative standard deviation for $n = 3$

ion were selected as possible interfering species, which may preconcentrated on the electrode surface through π-interaction or electrostatic attraction. The effects of several possible interfering substances were measured in phosphate buffer containing 25 μM BPA (Table 2). It is found that 100-fold concentration increase of Fe^{3+}, Al^{3+}, Mg^{2+}, $SO4^{2-}$ and Cl^{-}, and 50-fold concentration increase of phenol, catechol, resorcinol, hydroquinone and 4-nitrophenol have no influence on BPA detection with the I_{pa} variations below ±5%.

Real sample analysis

To check the applicability of N-G/M-GCE in real samples, commercially available goods (three polycarbonate plastic bottles and one receipt) were used as the experimental samples. The quantities of BPA were examined by the standard addition method, and the results are listed in Table 3. The recoveries are in the range of 99.1%–101.4%, so the fabricated sensor can be satisfied with the practical application.

Conclusions

In summary, N-G/M composite modified GCE has been successfully fabricated to detect trace BPA. Ascribed to the electrochemical conductivity and adsorption capacity of N-G/M, the sensor exhibits a good current response for the oxidation of BPA with a wide linear range and low detection limit. Moreover, the prepared sensor is proved to be suitable for real sample determination. Further study is needed to focus on applying the sensor on more complex targets, including samples taken from outdoor rivers, lakes, etc.

Acknowledgments The authors are grateful to the financial support of the National Nature Science Foundation of China (Nos. 51572036, 51472035), the Science and Technology Department of Jiangsu Province (BY2015027-18, BY2016029-12), Changzhou key laboratory of graphene-based materials for environment & safety (CE20160001-2, CM20153006) and the PAPD of Jiangsu Higher Education Institution.

Compliance with ethical standards The author(s) declare that they have no competing interests.

References

1. Fan J, Guo H, Liu G, Peng P (2007) Simple and sensitive fluorimetric method for determination of environmental hormone bisphenol a based on its inhibitory effect on the redox reaction between hydroxy radical and rhodamine 6G. Anal Chim Acta 585:134–138
2. Kuklenyik Z, Ekong J, Cutchins CD, Needham LL, Calafat AM (2003) Simultaneous measurement of urinary bisphenol a and alkylphenols by automated solid-phase extractive derivatization gas chromatography/mass spectrometry. Anal Chem 75:6820–6825
3. Sambe H, Hoshina K, Hosoya K, Haginaka J (2005) Direct injection analysis of bisphenol a in serum by combination of isotope imprinting with liquid chromatography-mass spectrometry. Analyst 130:38–40
4. Alkasir RS, Ganesana M, Won YH, Stanciu L, Andreescu S (2010) Enzyme functionalized nanoparticles for electrochemical biosensors: a comparative study with applications for the detection of bisphenol a. Biosens Bioelectron 26:43–49
5. Ragavan KV, Rastogi NK, Thakur MS (2013) Sensors and biosensors for analysis of bisphenol-a. TrAC Trends Anal Chem 52:248–260
6. Yin H, Zhou Y, Ai S, Han R, Tang T, Zhu L (2010) Electrochemical behavior of bisphenol a at glassy carbon electrode modified with gold nanoparticles, silk fibroin, and PAMAM dendrimers. Microchim Acta 170:99–105
7. Gao Y, Cao Y, Yang D, Luo X, Tang Y, Li H (2012) Sensitivity and selectivity determination of bisphenol a using SWCNT-CD conjugate modified glassy carbon electrode. J Hazard Mater 199-200: 111–118
8. Baghayeri M, Sedrpoushan A, Mohammadi A, Heidari M (2017) A non-enzymatic glucose sensor based on NiO nanoparticles/functionalized SBA 15/MWCNT-modified carbon paste electrode. Ionics 23:1553–1562
9. Baghayeri M, Veisi H (2015) Fabrication of a facile electrochemical biosensor for hydrogen peroxide using efficient catalysis of hemoglobin on the porous Pd@Fe3O4-MWCNT nanocomposite. Biosens Bioelectron 74:190–198
10. Baghayeri M, Ansari R, Nodehi M, Razavipanah I, Veisi H (2018) Label-free electrochemical bisphenol a aptasensor based on designing and fabrication of a magnetic gold nanocomposite. Electroanal 30:2160–2166
11. Baghayeri M (2017) Pt nanoparticles/reduced graphene oxide nanosheets as a sensing platform: application to determination of droxidopa in presence of phenobarbital. Sensor Actuat B-Chem 240:255–263
12. Jiao S, Jin J, Wang L (2014) Tannic acid functionalized N-doped graphene modified glassy carbon electrode for the determination of bisphenol a in food package. Talanta 122:140–144
13. Shen R, Zhang W, Yuan Y, He G, Chen H (2015) Electrochemical detection of bisphenol a at graphene/melamine nanoparticle-modified glassy carbon electrode. J Appl Electrochem 45:343–352

14. Zhang Y, Cheng Y, Zhou Y, Li B, Gu W, Shi X, Xian Y (2013) Electrochemical sensor for bisphenol a based on magnetic nanoparticles decorated reduced graphene oxide. Talanta 107:211–218
15. Liu C, Zhang AY, Si Y, Pei DN, Yu HQ (2017) Photochemical antifouling approach for electrochemical pollutant degradation on facet-tailored TiO2 single crystals. Environ Sci Technol 51: 11326–11335
16. Singh N, Reza KK, Ali MA, Agrawal VV, Biradar AM (2015) Self assembled DC sputtered nanostructured rutile TiO2 platform for bisphenol a detection. Biosens Bioelectron 68:633–641
17. Hummers WS, Offeman RE (1958) Preparation of graphitic oxide. J Am Chem Soc 80:1339
18. Sathish M, Mitani S, Tomai T, Honma I (2014) Supercritical fluid assisted synthesis of N-doped graphene nanosheets and their capacitance behavior in ionic liquid and aqueous electrolytes. J Mater Chem A 2:4731–4738
19. Kuramitz H, Nakata Y, Kawasaki M, Tanaka S (2001) Electrochemical oxidation of bisphenol a. application to the removal of bisphenol a using a carbon fiber electrode. Chemosphere 45: 37–43
20. Kurbanoglu S, Ozkan SA (2018) Electrochemical carbon based nanosensors: a promising tool in pharmaceutical and biomedical analysis. J Pharm Biomed Anal 147:439–457
21. Chen J, Li Y, Lv K, Zhong W, Wang H, Wu Z, Yi P, Jiang J (2016) Cyclam-functionalized carbon dots sensor for sensitive and selective detection of copper(II) ion and sulfide anion in aqueous media and its imaging in live cells. Sensor Actuat B-Chem 224:298–306
22. Chen H, Müller MB, Gilmore KJ, Wallace GG, Li D (2008) Mechanically strong, electrically conductive, and biocompatible graphene paper. Adv Mater 20:3557–3561
23. Fan H, Li Y, Wu D, Ma H, Mao K, Fan D, Du B, Li H, Wei Q (2012) Electrochemical bisphenol a sensor based on N-doped graphene sheets. Anal Chim Acta 711:24–28
24. Wang B, Qin Y, Tan W, Tao Y, Kong Y (2017) Smartly designed 3D N-doped mesoporous graphene for high-performance supercapacitor electrodes. Electrochim Acta 241:1–9
25. Panchakarla LS, Govindaraj A, Rao CN (2007) Nitrogen-and boron-doped double-walled carbon nanotubes. ACS Nano 1:494–500
26. Naderi HR, Sobhaninasab A, Rahiminasrabadi M, Ganjali MR (2017) Decoration of nitrogen-doped reduced graphene oxide with cobalt tungstate nanoparticles for use in high-performance supercapacitors. Appl Surf Sci 423:1025–1034
27. Ahmed J, Rahman MM, Siddiquey IA, Asiri AM, Hasnat MA (2017) Efficient bisphenol-a detection based on the ternary metal oxide (TMO) composite by electrochemical approaches. Electrochim Acta 246:597–605
28. Yin HS, Zhou YL, Ai SY (2009) Preparation and characteristic of cobalt phthalocyanine modified carbon paste electrode for bisphenol a detection. J Electroanal Chem 626:80–88
29. Jin GP, Yu B, Yang SZ, Ma HH (2011) Extremely sensitive electrode for melamine using a kind of molecularly imprinted nanoporous film. Microchim Acta 174:265–271
30. Anson FC (1964) Application of potentiostatic current integration to the study of the adsorption of cobalt(III)-(ethylenedinitrilo(tetraacetate) on mercury electrodes. Anal Chem 36: 932–934
31. Velasco JG (1997) Determination of standard rate constants for electrochemical irreversible processes from linear sweep voltammograms. Electroanal 9:880–882
32. Fan H, Li Y, Wu D, Ma H, Mao K, Fan D, Du B, Li H, Wei Q (2012) Electrochemical bisphenol a sensor based on N-doped graphene sheets. Anal Chim Acta 711:24–28
33. Peng J, Feng Y, Han XX, Gao ZN (2016) Simultaneous determination of bisphenol a and hydroquinone using a poly(melamine) coated graphene doped carbon paste electrode. Microchim Acta 183: 2289–2296
34. Zhan T, Song Y, Tan Z, Hou W (2017) Electrochemical bisphenol a sensor based on exfoliated Ni2Al-layered double hydroxide nanosheets modified electrode. Sensor Actuat B-Chem 238:962–971
35. Chen WY, Mei LP, Feng JJ, Yuan T, Wang AJ, Yu H (2015) Electrochemical determination of bisphenol a with a glassy carbon electrode modified with gold nanodendrites. Microchim Acta 182: 703–709